Influence of surface preparation on atomic layer deposition of Pt films*

Ge Liang(葛亮)[1], Hu Cheng(胡成)[1], Zhu Zhiwei(朱志炜)[1], Zhang Wei(张卫)[1], Wu Dongping(吴东平)[1,†], and Zhang Shili(张世理)[1,2]

[1]State Key Laboratory of ASIC and System, School of Microelectronics, Fudan University, Shanghai 200433, China
[2]Solid-State Electronics, the Ångström Laboratory, Uppsala University, Box 534, 75121 Uppsala, Sweden

Abstract: We report Pt deposition on a Si substrate by means of atomic layer deposition (ALD) using (methylcyclopentadienyl) trimethylplatinum ($CH_3C_5H_4Pt(CH_3)_3$) and O_2. Silicon substrates with both HF-last and oxide-last surface treatments are employed to investigate the influence of surface preparation on Pt-ALD. A significantly longer incubation time and less homogeneity are observed for Pt growth on the HF-last substrate compared to the oxide-last substrate. An interfacial oxide layer at the Pt–Si interface is found inevitable even with HF treatment of the Si substrate immediately prior to ALD processing. A plausible explanation to the observed difference of Pt-ALD is discussed.

Key words: Pt; atomic layer deposition; surface treatment; interfacial oxide layer
DOI: 10.1088/1674-4926/33/8/083003 **EEACC:** 2570

1. Introduction

Films having excellent conformation and large area uniformity can be grown by means of atomic layer deposition (ALD)[1]. Basically a chemical reaction process, ALD proceeds in a layer-by-layer control manner, based on the foundation of splitting a binary reaction into two half-reactions and alternating the exposure of the gas phase precursors for each half-reaction to a targeted surface[2]. The film growth is controlled by saturative precursor chemisorptions on the growth surface or by saturative reactions of the precursor with reactive surface groups making the process self-limiting. Once the deposition is approaching the surface saturation, the process becomes insensitive to small changes of the precursor dose. Hence, the thickness of the deposited films can be controlled accurately simply by altering the cycles of the deposition.

Several ALD processes for different noble metals, such as Pt[3,4], Ru[5], Rh[6], Pd[7], and Ir[8], have been investigated in recent years. Those noble metals, especially Pt, are candidate materials in applications such as capacitor electrodes in dynamic random access memories and ferroelectric random access memories[9]. Platinum growth by ALD is also well known for having attractive properties for its potential use in many applications concerning nanoscale structures. For instance, Pt nano-particles grown by ALD are being studied for use in nano-crystal nonvolatile memory applications[10]. Because of its large work function, Pt by ALD is also appropriate to be used as a band edge metal gate with high-k dielectrics in metal oxide semiconductor field effect transistors (MOSFET)[11]. Platinum is also widely used in fuel cells owing to its high catalytic activity[12]. Additionally, Pt can easily form Pt-silicide in the presence of Si and therefore Pt by ALD could be suitable for potential use in the source/drain region of future nano-scale MOS transistors in which ultra-shallow junctions are required[13].

Recently, it has been reported that Pt by ALD can be successfully grown by using (methylcyclopentadienyl) trimethylplatinum ($CH_3C_5H_4Pt(CH_3)_3$) and O_2 as precursor gases[3,4]. An extensive investigation of the interface between the grown Pt film and the substrate as well as of the dependence of Pt growth on substrate surface preparation is therefore highly desirable. Compared with a conventional physical vapor deposition processes, ALD process is very sensitively dependent on the conditions of the substrate surface. In this paper, the influence of surface preparation on ALD of Pt films is carefully investigated. A model of ALD of Pt films on a Si substrate using $CH_3C_5H_4Pt(CH_3)_3$ and O_2 as the precursor gases is proposed.

2. Experiments

Silicon wafers, (100)-oriented and p-type with a resistivity of 8–12 Ω·cm, are used as substrates for the experiments carried out in this paper. Since ALD process is very sensitive to the conditions of the initial surface of the substrate, two kinds of Si surfaces are prepared. The first kind of Si samples, HF-last, receives a surface clean in dilute HF solution (1 : 50) prior to wafer loading for Pt deposition immediately after the standard RCA cleaning procedure, in order to remove native oxide or chemical oxide on the Si surface. The HF-cleaned Si wafers are blown dry by N_2 gas. The second kind of Si samples, oxide-last, is thermally oxidized in dry O_2 at 1000 ℃ for 3 min to intentionally grow a high-quality thin oxide layer on the Si surface. The thickness of the grown thermal oxide is measured to be 5 nm by ellipsometry. Notably, to ensure that Pt would be deposited under identical conditions on the aforementioned two sample sets, both HF-last and oxide-last samples are loaded and processed at the same time.

* Project supported by the National S&T Major Project 02 (No. 2009ZX02035-003), the National Natural Science Foundation of China (No. 61176090), and the Program for Professor of Special Appointment (Eastern Scholar) at Shanghai Institutions of Higher Learning.
† Corresponding author. Email: dongpingwu@fudan.edu.cn
Received 11 February 2012, revised manuscript received 10 April 2012

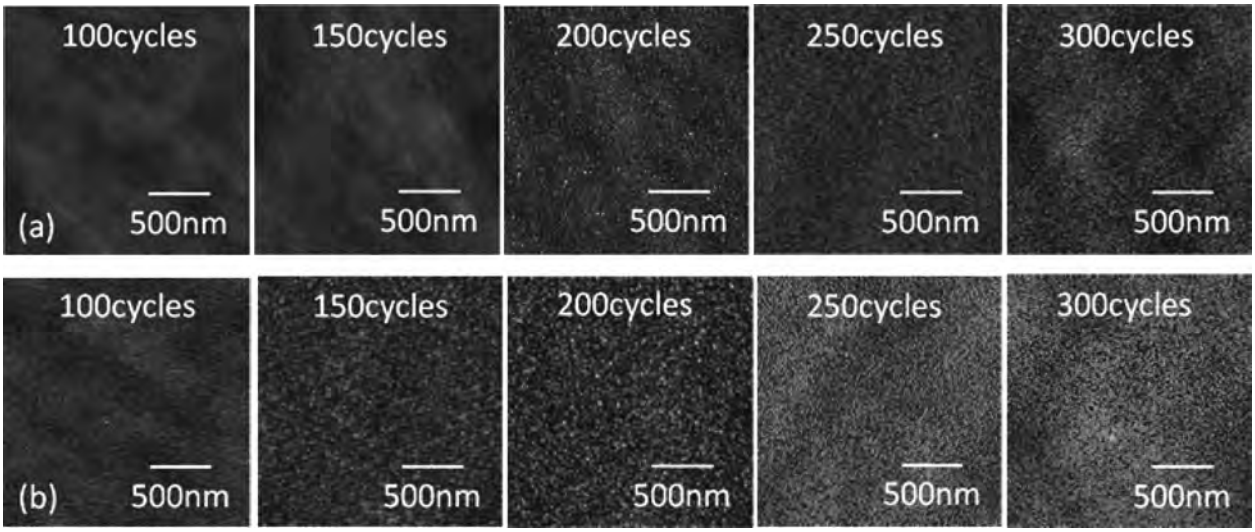

Fig. 1. AFM images of Pt-ALD on (a) HF-last and (b) oxide-last surfaces after different cycles of deposition.

The Pt deposition is carried out in a Beneq TFS200-125 ALD tool using $CH_3C_5H_4Pt(CH_3)_3$ and O_2 as the precursor gases. The $CH_3C_5H_4Pt(CH_3)_3$ precursor is heated to 70 ℃ while the temperature in the ALD chamber is kept at 300 ℃. According to previous reports, if the deposition temperature was set at 300–350 ℃, mirror-like Pt films could be obtained[3]. When the growth temperature was 350 ℃, Pt was deposited on the chamber walls of the Pt precursor inlet tube, indicating that the Pt-precursor thermally could decompose at this specific temperature. On the other hand, since only very thin films could be obtained at 250 ℃, the chamber temperature is set at 300 ℃ in our experiments in order to have a controllable self-limiting process. The deposition further uses O_2 gas as the oxygen supplying agent and gaseous N_2 for purging the reactor during the deposition process. The pressure during ALD processing is kept at 130 Pa. The process parameters for Pt-ALD are listed as follows: Pulse1 ($CH_3C_5H_4Pt(CH_3)_3$): 1 s, Purge1 (N_2): 3 s, Pulse2 (O_2): 160 ms, and Purge2 (N_2): 10 s. The physical and electrical properties of the deposited films are analyzed by atomic force microscopy (AFM), scanning electron microscopy (SEM), X-ray photoelectron spectroscopy (XPS) and transmission electron microscopy (TEM).

3. Results and discussions

Micro-images of the surface of the two kinds of samples with various ALD cycles of Pt growth obtained by AFM are shown in Fig. 1. The Pt growth on the HF-last surface is observed to be significantly retarded compared with that on the oxide-last surface. As can be seen clearly, the presence of Pt particles on the oxide-last surface is already weakly detectable after 100 cycles of deposition and they become clearly visible after 150 cycles. However, Pt particles can hardly be detected on the HF-last surface until about 200 cycles, indicating that there is a significant incubation period for Pt-ALD on a Si surface.

In order to gain a deeper understanding of the Pt growth, root-mean-square (RMS) values are obtained to quantify the surface roughness for the aforementioned AFM samples. As

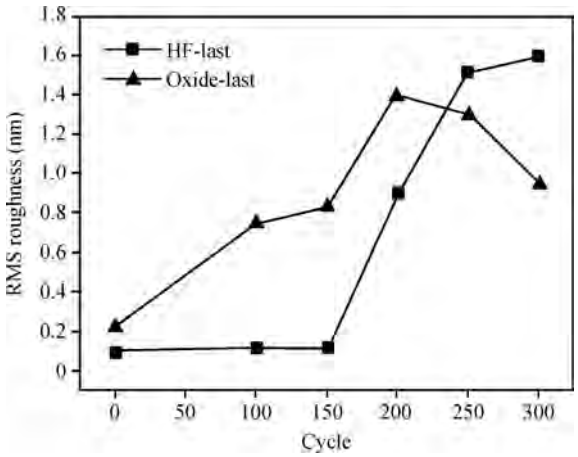

Fig. 2. Variation of RMS values with ALD cycle count for growth of Pt on HF-last and oxide-last surfaces.

can be seen in Fig. 2, an increase in the ALD cycle count is accompanied by a continual increase in RMS value for the HF-last samples. Thereafter, it drops when the cycle count increases above 200. The observations can be understood by referring to a typical three-step growth model: nucleation, subsequent grain coarsening, followed by vertical thickening. For the HF-last samples, the Pt growth is apparently mostly confined during the first two steps of nucleation and grain coarsening. The initial low RMS values at 100 and 150 cycles are obviously a consequence of the severely retarded Pt nucleation. Once nucleated, the rapid increase in RMS value above 150 cycles is a signature of continuous grain coarsening. However, coalition of the discrete Pt particles/grains seems incomplete even after 300 cycles of Pt-ALD processing. For the oxide-last samples, the initial RMS value at 100 cycles is already rather high, indicating a much easier Pt nucleation compared to that on the HF-last surface. This is followed by grain coarsening until the ALD cycle count reaches 200. Thereafter, the decrease in RMS value corresponds to a vertical thickening of a continuous film. The discussion is supported by the SEM and TEM

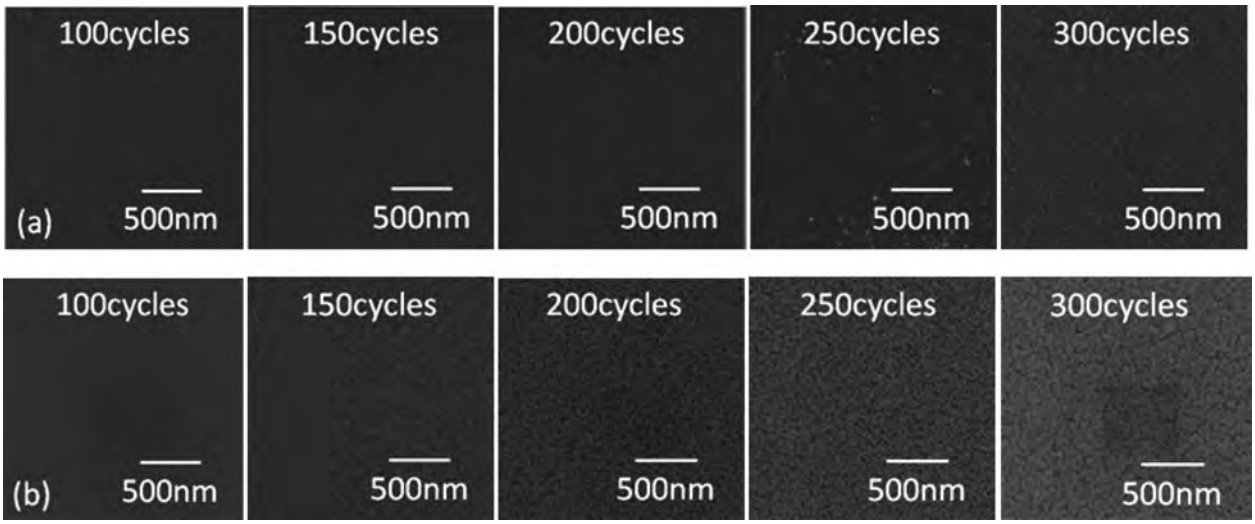

Fig. 3. SEM images of Pt-ALD on (a) HF-last and (b) oxide-last surfaces after different cycles of deposition.

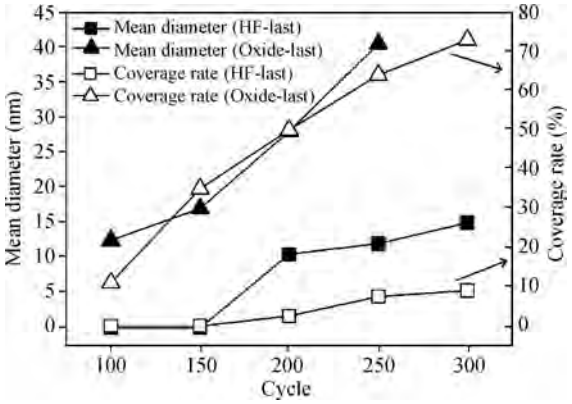

Fig. 4. Mean diameter of Pt particles and blocks and coverage rate of Pt for all samples prepared.

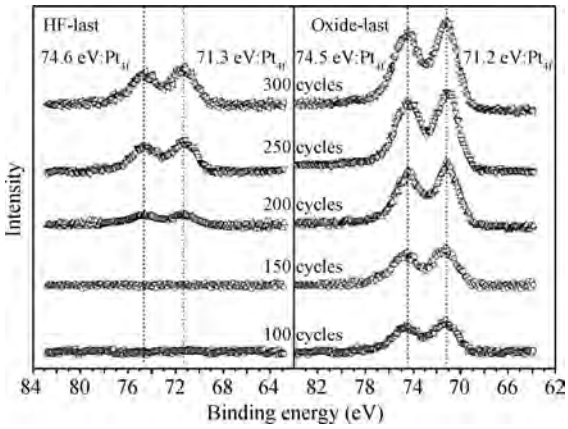

Fig. 5. XPS data of Pt-ALD on HF-last (left panel) and oxide-last (right panel) substrates.

data shown below.

Micrographs of SEM in Fig. 3 demonstrate a more obvious and persuasive comparison of Pt growth on the two kinds of substrates. On the oxide-last surface, densely nucleated Pt particles are already clearly observable after 150 cycles of ALD processing. The particles or grains continually grow and merge with one another with increasing cycle counts. For the sample with a 300 cycle count, a continuous Pt film is achieved. However, sparsely distributed Pt grains are observed for the HF-last sample until 200 cycles. Even after 300 cycles, the Pt grains remain largely separated.

Image-pro plus, a powerful 2D and 3D image processing and analysis software[14], is used to obtain the mean diameter and number of the Pt particles and blocks deposited on the samples. The mean diameter is shown in Fig. 4. It can be seen that almost no Pt is deposited on the HF-last substrate as long as the cycle count is no larger than 150. Moreover, with the same cycle count the diameter of the particles of the HF-last samples is significantly smaller than that of the oxide-last samples. For the oxide-last samples, Pt particles with a diameter larger than 10 nm are already visible after 100 cycles of ALD and the diameter increases drastically with increasing cycle count. Coverage rate, defined as the ratio of the summed Pt-covered area to the total selected surface area, is shown for the samples in Fig. 4. The coverage ratio for the oxide-last sample at 300 cycle count already surpasses 70%, while that for the HF-last sample for the same cycle count is still less than 10%. Hence, it is confirmed that the Pt nucleation and growth on the oxide-last surface is much easier than those on the HF-last surface.

The Pt-ALD films on both kinds of substrates are examined by XPS and the results are shown in Fig. 5. For both sample sets, the intensity of the Pt4f peaks increases with increasing cycle count, indicating an increase of Pt density or thickness, and hence the particle size[10]. According to the XPS data, the Pt being deposited can be identified as elemental metallic Pt[10,15−17]. In detail, stronger elemental Pt peaks are found overall for the oxide-last samples rather than the HF-last ones. No Pt peaks can be found on the HF-last samples with cycle counts of 100 and 150. The XPS results are consistent with the AFM and SEM results presented earlier.

The samples with cycle counts of 200 and 300 are analyzed using TEM and the results are shown in Fig. 6. In accordance with the aforementioned AFM and SEM results, the Pt particles on the oxide-last substrate are substantially larger in size and

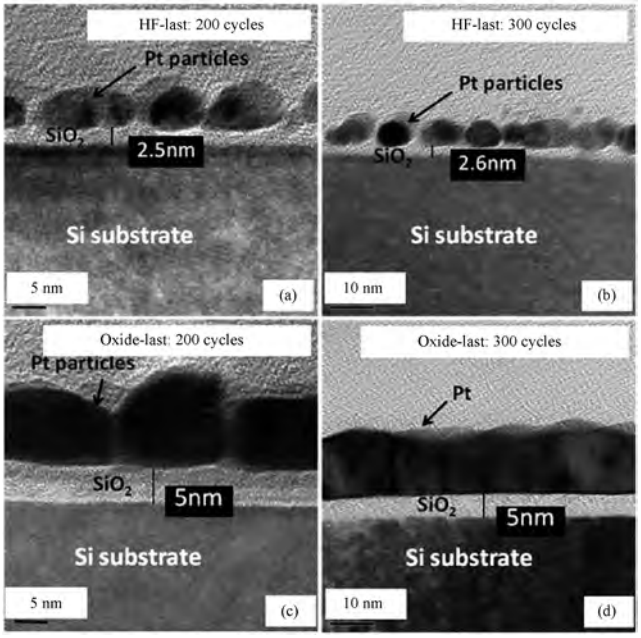

Fig. 6. Cross-sectional TEM micrographs for substrates (a, b) HF-last and (c, d) oxide-last.

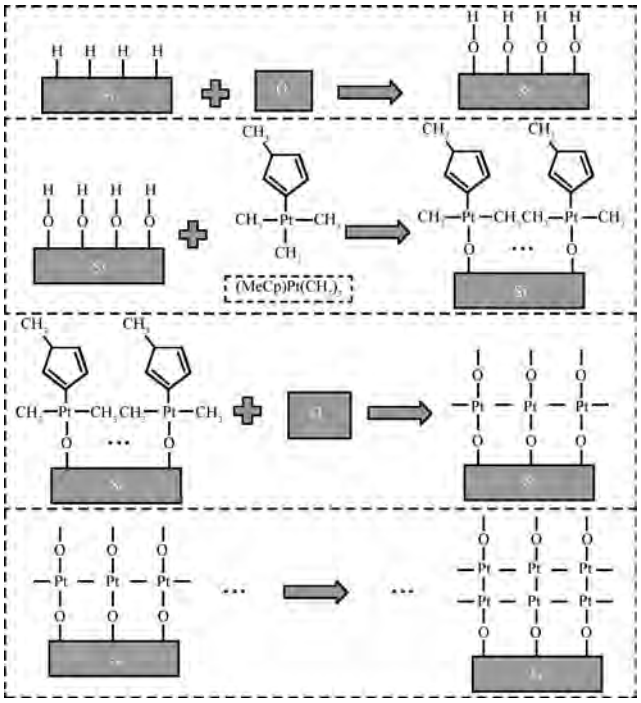

Fig. 7. Schematic representation of Pt-ALD on an HF treated Si surface.

denser than those on the HF-last substrate. At 200 cycles, the diameter of the Pt particles on the oxide-last substrate is around 10 nm, which is twice that on the HF-last substrate. An interfacial oxide layer about 2.5 nm in thickness is clearly observed on the HF-last substrate, while it is roughly 5 nm for the oxide-last substrate. The latter is identical to the thickness of the oxide layer grown originally. The former 2.5 nm thick oxide layer is most likely formed during the ALD process at 300 ℃, since after HF treatment the regrown native oxide is measured to be around 1.5 nm thick after exposure for a few hours under ambient conditions. Furthermore, the presence of Pt could enhance Si oxidation, since it is known that noble metals can act as a catalyst during the metal-promoted oxidation[18, 19] and oxygen can easily diffuse through a Pt film and reach the underlying Si surface, forming an oxide layer at the Pt–Si interface[20].

A plausible explanation to the observed difference in Pt-ALD on the HF-last versus oxide-last surfaces is discussed as follows, with reference to Fig. 7 for a schematic representation of Pt-ALD on the HF-last surface. For the oxide-last samples, the surface is terminated with –O or –OH which can easily be broken off the surface[21]. When $CH_3C_5H_4Pt(CH_3)_3$ is introduced to the surface, it loses one of its three CH_3 radicals and is adsorbed on the O dangling bond. During the next O_2 pulse, the Pt surface becomes terminated with O, leaving the surface prepared for the next ALD cycle[22,23]. Hence, as the ALD cycles repeat, the Pt growth proceeds in a layer-by-layer manner. For the HF-last sample, after the HF-last process step, the Si surface is terminated with chemically stable Si–H bonds which are very difficult to break up to yield Si dangling bonds[24,25]. Hence, absorption of $CH_3C_5H_4Pt(CH_3)_3$ and subsequent nucleation of Pt on the Si surface are inhibited. The subsequent repetition of O_2 exposure during ALD cycling could gradually convert the Si–H bonds to the Si–OH bonds, thereby facilitating the $CH_3C_5H_4Pt(CH_3)_3$ absorption and Pt nucleation. Consequently, a significantly longer incubation time and less homogeneous growth for Pt deposition occur on the HF-last surface. Not only can O_2 convert the Si–H bonds to Si–OH bonds, but can also easily reach the underlying Si substrate forming an oxide layer even after a Pt film has been deposited[20]. Notably, the schematic representation of Pt-ALD on the HF-last surface is a simplified explanation for platinum growth and interfacial oxide layer is not shown.

4. Conclusions

Platinum deposition on a Si substrate by means of ALD is found to be sensitively dependent on the surface conditions. On the oxide-last surface, Pt growth is already clearly detectable after 100 cycles of deposition and a ∼10 nm thick relatively continuous layer Pt is found after 300 cycles. In contrast, on the HF-last surface, Pt growth is significantly retarded and only discrete Pt particles are formed even after 300 cycles of deposition. Ascribed to difficulties in breaking the Si-H bonds, absorption of the Pt precursor can hardly be realized on the HF-last surface. While continuous O_2 pulses can create –O dangling bonds or –OH groups which would favor absorption of the Pt precursor and hence Pt ALD, it also results in a ∼2.5 nm thick interfacial oxide layer through the oxidation process.

References

[1] Puurunen R L. Surface chemistry of atomic layer deposition: a case study for the trimethylaluminum/water process. J Appl Phys, 2005, 97: 121301

[2] Kim D J, Dunn B C, Huggins F, et al. SBA-15-supported iron catalysts for Fischer-Tropsch production of diesel fuel. Energy & Fuels, 2006, 20: 2608

[3] Aaltonen T, Ritala M, Sajavaara T, et al. Atomic layer deposition of platinum thin films. Chem Mater, 2003, 15: 1924

[4] Aaltonen T, Ritala M, Tung Y L, et al. Atomic layer deposition of noble metals: exploration of the low limit of the deposition temperature. Mater Res, 2004, 19: 3353
[5] Aaltonen T, Alén P, Ritala M, et al. Ruthenium thin films grown by atomic layer deposition. Chem Vap Deposition, 2003, 9: 45
[6] Aaltonen T, Ritala M, Leskelä M, et al. ALD of rhodium thin films from Rh(acac)3 and oxygen. Electrochem Solid-State Lett, 2005, 8: C99
[7] Eyck G A T, Pimanpang S, Bakhru H, et al. Atomic layer deposition of Pd on an oxidized metal substrate. Chem Vap Deposition, 2006, 12: 290
[8] Aaltonen T, Ritala M, Sammelselg V, et al. Atomic layer deposition of iridium thin films. J Electrochem Soc, 2004, 151: G489
[9] Bandaru J, Sands T, Tsakalakos L. Simple Ru electrode scheme for ferroelectric (Pb,La)(Zr,Ti)O_3 capacitors directly on silicon. J Appl Phys, 1998, 84: 1121
[10] Novak S, Lee B, Yang X, et al. Platinum nanoparticles grown by atomic layer deposition for charge storage memory applications. J Electrochem Soc, 2010, 157: H589
[11] Wilk G D, Wallace R M, Anthony J M. Hafnium and zirconium silicates for advanced gate dielectrics. J Appl Phys, 2000, 87: 484
[12] Jiang X, Huang H, Prinz F B, et al. Application of atomic layer deposition of platinum to solid oxide fuel cells. Chem Mater, 2008, 20: 3897
[13] Faber E J, Wolters R A M, Schmitz J. On the kinetics of platinum silicide formation. Appl Phys Lett, 2011, 98: 082102
[14] Biehlmaier O, Hehl J, Csucs G. Acquisition speed comparison of microscope software programs. Microsc Res Tech, 2011, 74: 539
[15] NIST X-ray Photoelectron Spectroscopy Database
[16] Lewera A, Zhou W P, Vericat C, et al. XPS and reactivity study of bimetallic nanoparticles containing Ru and Pt supported on a gold disk. Electrochimica Acta, 2006, 51: 3950
[17] Kiss G, Varhegyi E B, Mizsei J, et al. Examination of the CO/Pt/Cu layer structure with Kelvin probe and XPS analysis. Sensors and Actuators B, 2000, 68: 240
[18] Hiraki A, Lugujjo E, Mayer J W. Formation of silicon oxide over gold layers on silicon substrates. J Appl Phys, 1972, 43: 3643
[19] Namba K, Yuasa T, Nakato Y. Effect of chemical oxide layers on platinum-enhanced oxidation of silicon. J Appl Phys, 1997, 81: 7006
[20] Shi J, Kojima D, Hashimoto M. The interaction between platinum films and silicon substrates: effects of substrate bias during sputtering deposition. J Appl Phys, 2000, 88: 1679
[21] McCormick J A, Rice K P, Paul D F, et al. Analysis of Al_2O_3 atomic layer deposition on ZrO_2 nanoparticles in a rotary reactor. Chem Vap Deposition, 2007, 13: 491
[22] Li J H, Li X H, King D M, et al. Highly dispersed Pt nanoparticle catalyst prepared by atomic layer deposition. Appl Catal B: Environ, 2010, 97: 220
[23] Hiratani M, Nabatame T, Matsui Y, et al. Platinum film growth by chemical vapor deposition based on autocatalytic oxidative decomposition. J Electrochem Soc, 2001, 148: C524
[24] Grundner M, Jacob H. Investigations on hydrophilic and hydrophobic silicon (100) wafer surfaces by X-ray photoelectron and high-resolution electron energy loss-spectroscopy. Appl Phys A, 1986, 39: 73
[25] Yao H, Woollam J A. Spectroscopic ellipsometry studies of HF treated Si (100) surfaces. Appl Phys Lett, 1993, 62: 3324